LAMININ MICRODROPLET DEPOSITION ON CONDUCTING POLYMER FILMS FOR NEURAL REGENERATION

A Thesis

Presented to

the Faculty of the Department of Biomedical Engineering

University of Houston

In Partial Fulfillment

of the Requirements for the Degree

Master of Science

in Biomedical Engineering

by

Kartik Sharma

May 2019

LAMININ MICRODROPLET DEPOSITION ON CONDUCTING POLYMER FILMS FOR NEURAL REGENERATION

Kartik Sharma

Approved:

Chair of the Committee
Mohammad Reza Abidian, Associate Professor,
Biomedical Engineering Department

Committee Members:

Sheereen Majd, Assistant Professor,
Biomedical Engineering Department

Tianfu Wu, Assistant Professor,
Biomedical Engineering Department

Suresh K. Khator, Associate Dean,
Cullen College of Engineering

Metin Akay, Professor and Chair,
John S. Dunn Endowed Chair,
Department of Biomedical Engineering

ACKNOWLEDGEMENTS

I would like to thank my advisor, Dr. Mohammad Reza Abidian, for providing me the opportunity to work in his laboratory and for morally supporting me throughout the project. I would also like to thank my committee members, Dr. Sheereen Majd and Dr. Tianfu Wu, for their valuable time in assessing the progress of my project and their cooperation in this endeavor. I thank all the past and present lab members for their guidance, assistance, and ideas for my thesis. I would also like to give a special thanks to Mr. Omid Dadras with whom I was able to work on a related project which helped me to sort out several problems in my project.

Finally, I must thank my friends and family. Without their love, patience, motivation, and support, I would not have managed to come this far. The space allotted for acknowledgement in this report limits my expression of gratitude for you all. However, making the best use of opportunity and space I would again like to thank all the above-mentioned people for everything they have done for me.

To my mother, Sanju Sharma, for her ongoing love, support, and patience.

LAMININ MICRODROPLET DEPOSITION ON CONDUCTING POLYMER FILMS FOR NEURAL REGENERATION

An Abstract

Of a

Thesis

Presented to

the Faculty of the Department of Biomedical Engineering

University of Houston

In Partial Fulfillment

of the Requirements for the Degree

Master of Science

in Biomedical Engineering

by

Kartik Sharma

May 2019

ABSTRACT

Conducting polymers are valuable tools in tissue engineering as they can play an important role in enhancing cellular response to guidance cues due to their electrical conductivity. Extracellular matrix proteins like laminin can provide a strong guidance cue to direct cellular regrowth. When combined, these two can prove to be unbeatable alternative for tissue regeneration applications. However, the biggest challenge lies in depositing these proteins on the surface of conducting polymer to get the best response out of neurons for neural regeneration. In this study, various parameters have been optimized to idealize the deposition of laminin on conducting polymer's surface. From this study, an optimized patterning technique can be established to deposit laminin on PEDOT substrates such that minimum volume of laminin is used, the pattern has very well-balanced distances between adjacent rows and columns, and there is least possible void space between the droplets both in horizontal and vertical directions.

TABLE OF CONTENTS

ACKNOWLEDGEMENTS iv

ABSTRACT vii

TABLE OF CONTENTS viii

LIST OF FIGURES ix

LIST OF TABLES xi

LIST OF ABBREVIATIONS xii

CHAPTER 1. Introduction 1

1.1 Background 1

1.2 ECM proteins in neural regeneration 3

1.3 Conducting polymers in neural regeneration 9

1.4 Objective of the thesis 11

CHAPTER 2. Materials and Methods 13

2.1 Materials 13

2.2 Printing Laminin on conducting polymer 13

2.2.1 Preparation of conducting polymer substrates 13

2.2.2 Preparation of Agarose hydrogel 15

2.2.3 Laminin printing and transferring to conducting polymer 16

2.3 Immunohistochemistry 17

CHAPTER 3. Results and discussions 18

CHAPTER 4. Conclusions and future work 37

REFERENCES 39

LIST OF FIGURES

		Page
FIGURE 1	Axonal response to homogenous and gradient distribution of growth cues	**3**
FIGURE 2	Model showing turning of growth cone towards gradient	**4**
FIGURE 3	Switching sensitivity of axons before and after crossing midline	**6**
FIGURE 4	Serpentine microfluidic channel to form laminin gradients	**7**
FIGURE 5	Microfluidic device that can generate multiple gradients by tuning flow rates of Laminin and BSA in adjacent channels	**8**
FIGURE 6	Schematics showing cellular response to neural-electrode insertion	**10**
FIGURE 7	Schematic representation of (A) gold coated substrate, and (B) electrodeposition process	**15**
FIGURE 8	Schematic representation of PEDOT coated substrate	**15**
FIGURE 9	PEDOT coated substrate soaked in 60µl PLL	**16**
FIGURE 10	Schematic arrangement of XYZ stage for printing Laminin on hydrogel	**16**
FIGURE 11	Schematic representation of soaking Laminin coated substrate in 60µl (A) BSA, (B) PAB, and (C) SAB	**17**
FIGURE 12	Laminin block (80µg/ml) with droplet volume of 17.5nl/s	**19**
FIGURE 13	Laminin Block (80µg/ml) with droplet volume of 10nl/s	**20**
FIGURE 14	Laminin block (100µg/ml) with different distances between droplets	**21**
FIGURE 15	Block of laminin (100µg/ml) showing (A) non-overlapping droplets, and (B) overlapping droplets	**21**

FIGURE 16	Laminin block (100µg/ml) with (A) a pattern, (B) diameter distribution, (C) corrected diameter distribution, and (D) intensity distribution for an Edge to Edge patterning	**22-23**
FIGURE 17	Laminin block (100µg/ml) with (A) pattern, (B) diameter distribution, (C) intensity distribution, (D) diameter comparison among patterns, and (E) intensity comparison among patterns for an Edge to Edge patterning	**24-25**
FIGURE 18	Pictorial representation of (A) Edge to Edge, and (B) Shifted patterning techniques	**26**
FIGURE 19	Laminin block (100µg/ml) with (A) a pattern, (B) diameter distribution, (C) corrected diameter distribution, and (D) intensity distribution for the Shifted patterning	**27-28**
FIGURE 20	Laminin block (100µg/ml) with (A) a pattern, (B) diameter distribution, and (C) intensity distribution for the Shifted patterning	**28-29**
FIGURE 21	Laminin block (100µg/ml) with (A) a pattern, (B) diameter distribution, and (C) intensity distribution for the Shifted patterning	**30-31**
FIGURE 22	Laminin block (100µg/ml) with (A) a pattern, (B) diameter distribution, and (C) intensity distribution, (D) diameter comparison, and (E) intensity comparison for the Shifted patterning	**31-33**
FIGURE 23	Representation of difference between the two types of pattering in terms of (A) laminin patterns, and (B) pictorial representations	**34**
FIGURE 24	(A) Inverted-V Laminin gradient (40-60-80-100-80-60-40µg/ml), (B) droplet diameter range, and (C) graph representing intensities in Laminin gradient for the Shifted patterning	**34-35**

LIST OF TABLES

		Page
TABLE 1	Comparison of the two Hamilton syringes used for experiments	**18**
TABLE 2	Parameters for Hamilton syringe with gauge #30	**19**

LIST OF ABBREVIATIONS

ECM	Extracellular matrix
CP	Conducting polymer
DI	De-ionized
SNR	Signal to noise ratio
SE	Source electrode
WE	Work electrode
EDOT	3,4-ethylenedioxythiophene
PEDOT	poly(3,4-ethylenedioxythiophene)
PSS	polystyrene sulfonate
PLL	Poly-L-lysine
BSA	Bovine serum albumin
PAB	Primary antibodies
SAB	Secondary antibodies
PBS	Phosphate-buffered saline
EVAP	Evaporative emission control system

CHAPTER 1. INTRODUCTION

1.1 Background

The nervous system is the controlling part of a living organism which is built up of two components: the central nervous system and the peripheral nervous system. The central nervous system further consists of the brain and spinal cord whereas, the peripheral nervous system is made up of nerves and specialized cells in the rest of the body. Communication between the two subparts is very important for the overall functioning of a living organism. This transfer of information takes place with the help of interconnections between specialized cells called neurons in both the systems. Ganglia or a cluster of sensory cells record signals coming from the outside world, convert them into nervous system understandable form and send them to different parts of the brain. Various parts of the brain are responsible for dealing with different situations and compare the input signals further feeding the peripheral system with an appropriate set of guidelines to take actions. This exchange of information is facilitated by a vast network of channels called axons.

Sometimes, the connections between these axons break due to a disease or physical damage which may lead to permanent loss of function of a specific body part or organ. Rebuilding these connections is as much necessary as their development during the embryonic growth in the first place. Many researchers have worked in this direction to come up with alternative approaches to fix hampered connections. The

science of axon regeneration focusses on manipulating projections tipped on axons called neuronal growth cones. When observed in embryos, it was found that the neurons extend their axons in the desired direction lead by growth cones. Growth cones respond to extracellular guidance cues which either attract or repel them. These cues have the capability to operate in both short and long distances (1). In response to these guidance molecules, growth cones select the path along which axons must navigate. It has been noted that these ECM biomolecules induce changes in the cytoskeleton dynamics of the growth cones by modulating gene expressions. Consequently, given such controlling ability, specific cues can control which axons respond to what cue and at what time. Such nature of this highly sophisticated guiding process is necessary to make sure that an axon which was attracted by a set of cues is repelled after crossing that zone so that it doesn't end up moving around the same locality.

When this cellular mechanism was first suggested (2), it was speculated that chemotropic biomolecules and other growth factors secreted by target tissues excite growth cones to navigate in the target direction. However, this theory was not practically validated until Lumsden and Davies (3) conducted an in vitro trial. In the experiment, they placed axon emitting tissue on one side and target tissue on the other. The space between the two was covered with collagen droplet, which served as a perfect medium for axon growth and stabilized the gradient on target tissue end. This arrangement was followed by Marc Tessier-Lavigne and others (4). They found out two molecules called netrins which in Sanskrit means guiding as the first chemotropic factors. Other growth factors involved in axon guidance have also been found (5).

1.2 ECM proteins in neural regeneration

Netrin-1, netrin-2, UNC-6, and Laminin are the few important among many ECM proteins to guide neural regeneration. However, one more interesting aspect surfaced during these experiments as shown in figure 1. Figure 1 shows the difference between the effects of homogenous distribution and gradient distribution of cues (left and right columns respectively) on outgrowth patterns of axons (2).

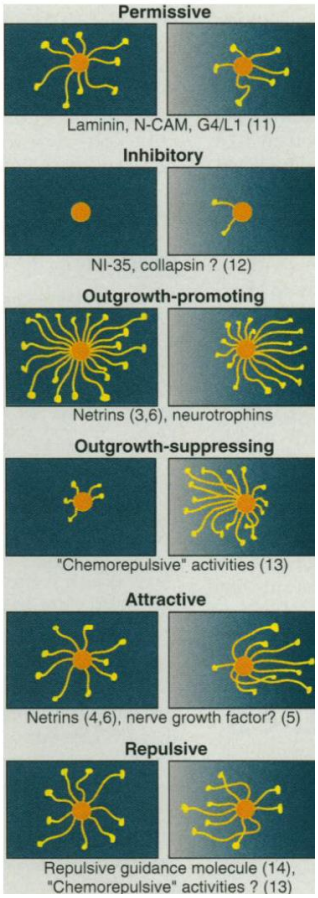

Figure 1. Axonal response to homogenous (left column) and gradient distribution (right column) of growth cues

It was observed (1) as shown in figure2 that with the homogenous molecule base, the axons grew equally in all directions and in the gradient of chemo-attractant molecules, they grew and increased in number towards higher concentration. On the contrary, in the presence of chemo-repulsive gradients, nerve growth took place towards the lower concentration.

The curiosity to understand how growth cones turn towards or away from these molecules lead to further investigations (6), which revealed their role in genetic manipulation of growth cones (7). Figure 2 shows the structure of growth cones built up of filopodium, a matrix of actin filaments and microtubule bundles.

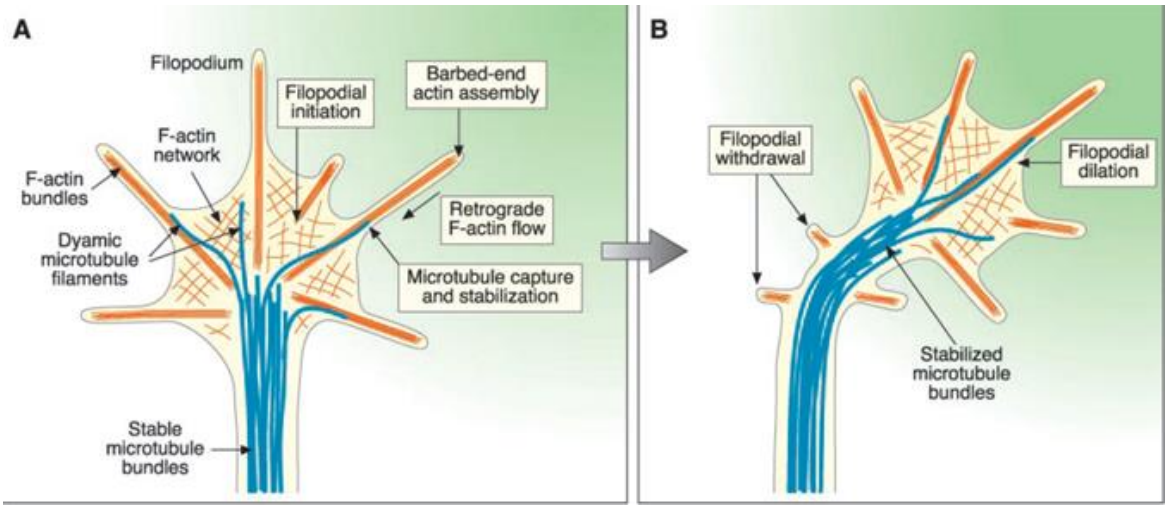

Figure 2. Model showing turning of growth cone towards gradient (green)

Filopodia can be interpreted as the leading elements which often extend asymmetrically before the growth cone turns (8) and have been thought of playing a crucial role in steering the growth cones (9) by generating mechanical force (10). Microtubule filaments extend into the peripheral regions of growth cones and their role in stabilizing filopodium is also important in growth cone turning in vivo (11). There are

numerous ways by which a guidance cue can initiate and promote growth cone steering. For example, prospective targets of signaling pathways are usually molecules like Arp2/3 which can nucleate new actin fibers and Ena/VASP proteins which further promote filopodial extensions etc. These proteins promote actin filament elongation by localizing in the leading edge of lamellipodia. When the concentration of these proteins decreases, it leads to shorter and more branched filaments which increase motility. On the contrary, when their concentration increases in the leading edge, it leads to longer and unbranched filaments which reduce motility.

Also, it is very interesting to note that growth cones switch their response to the same guidance cue. This unique nature was first quantified when commissural axons were seen to first get attracted towards the midline in the central nervous system and after crossing the midline, they switched their response by moving away from the midline and never turning back. Experiments showed that before crossing the midline, commissural axons were attracted by netrin (3) but did not respond to midline repellant called Slit. However, after crossing the midline, they become completely insensitive to netrins and are repelled by Slit. Therefore, the question becomes what exactly happened after crossing the midline? In flies, Robo receptors which are Slit receptors are up-regulated after axon crossing the midline only. The Robo receptors are down-regulated or not expressed when the axon has either not reached the midline or while it is crossing the midline (12). This explains for the switching behavior of axons as shown in figure 3 (1).

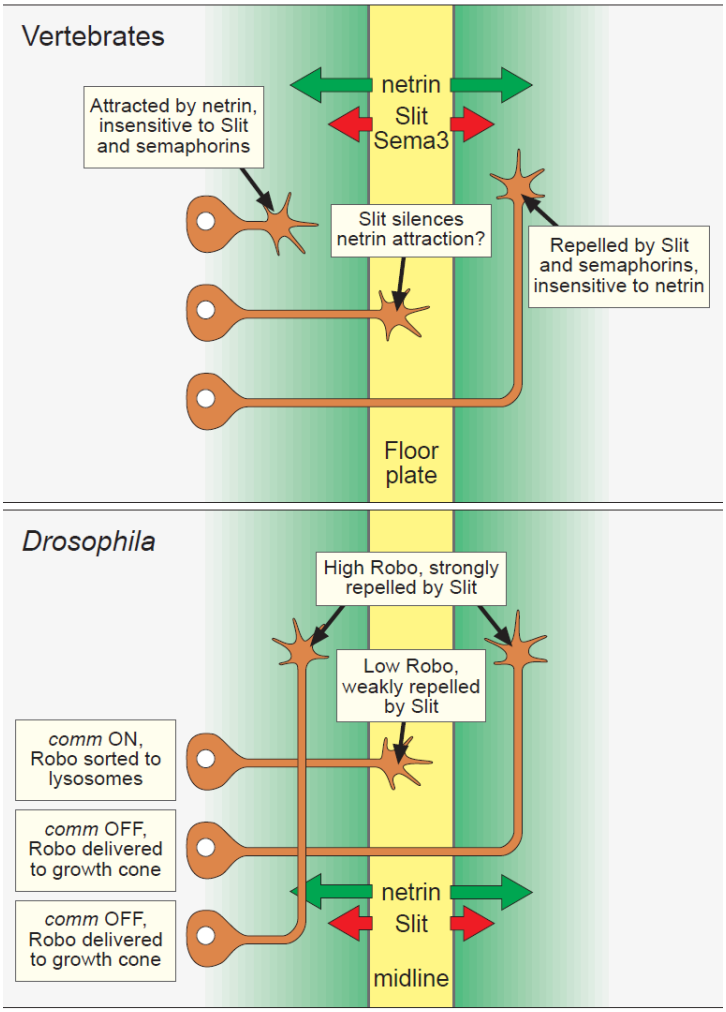

Figure 3. Switching sensitivity of axons before and after crossing midline

After the realization of the role of ECM molecules in neuronal development, several techniques using such natural phenomenon for artificial regeneration have come into the picture. Laminin, a very popular ECM protein has been widely exploited for attaining neurite growth under different conditions. Work (13) showed the role of ECM as a support structure in association with Laminin gradients to better the 3D neurite extension. In addition to researching the importance of 3D structure in enhancing regeneration, actual 3D structures like conduits coated with Laminin have also been developed to guide neuronal generation (14). These conduits not only

directed the dendrites in the desired direction but also channelized the flow of growth factors in the region where neural regrowth was required. On one hand, the concentration gradients of Laminin have been found to play a significant role in growth cone pathfinding, on the other hand, its pH has also been researched to impact neurite growth (15). Research showed that Laminin with acidic pH promoted neurite growth two folds better than Laminin with neutral pH.

Microfluidics has also been one of the major fields focusing on tissue engineering, especially neural engineering. Dertinger et al. used a microfluidic device to form a laminin gradient with BSA (3). The device (Figure 4) consisted of microchannels (3) which formed a uniform gradient with pure laminin on one side and pure BSA on the other. They found the axon orientation of hippocampal neurons towards the higher concentration of laminin.

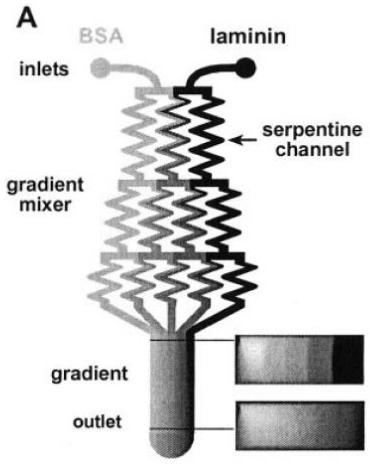

Figure 4. Serpentine microfluidic channel to form laminin gradients

One more innovative way (16) of quantitively analyzing axonal response to different slopes within one setup showed an increased axon guidance ratio with an

increased slope. Here, two asymmetrically designed peripheral channels (Figure 5) with opposite flow directions could generate numerous Laminin gradients with multiple slopes in the central channel (7). Therefore, it was relatively easy to compare the response of neurites extended by neurons partitioned with the Laminin gradients by just a porous membrane in the same setup towards different slopes.

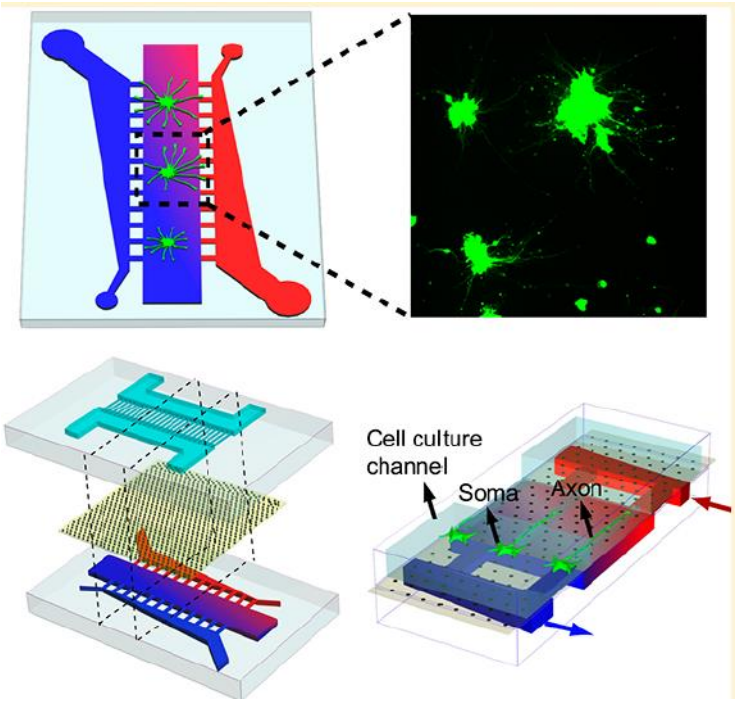

Figure 5. Microfluidic device that can generate multiple gradients by tuning flow rates of Laminin and BSA in adjacent channels

Microprinting which translates to the patterning of biomolecules that are believed to affect nerve growth also provides a handy tool to conduct neural regrowth research. A lot of research has already taken place involving the printing of proteins on the surface of biomaterials like conducting polymers etc. Micro-structuring techniques (17) to print substrate bound proteins have given a better understanding of axonal growth response to guidance cues. A study was conducted (18) to investigate the effect

of varying and constant concentrations of chemoattractive and chemorepulsive cues on neurons. Evidently, for chemoattractant molecules, neurons sent their dendrite towards higher concentration in the varying concentration arrangement while there was no directional specificity in case of constant concentration arrangement. In the case of chemorepulsive cues, there was no growth at all in both cases. Rita Fricke et al (19) tested the effect of supplementing Laminin with poly-L-lysine (PLL) on surface adherence of neurons, growth, and guidance of neurites. As a result, a combination of PLL and Laminin proved to be effective over only PLL coating on the surface of conducting polymers in all the 3 scenarios with best results for neural surface adherence.

1.3 Conducting polymers in neural regeneration

Biomaterials such as CP have also revolutionized the interaction with biological systems. The same nature of these biopolymers has been exploited by researchers to perform a vast range of neuronal interfacing including recording and stimulating neural activities, delivering drugs and biomolecules to target tissues for easing device-tissue interactions and neural regeneration (20). The main benefit of using CPs (1) for neural interfacing is that they may help in overcoming the problem of gliosis which is the foreign body response of tissues due to strain mismatch with metal electrodes (Figure 6). In gliosis, astrocytes, and microglia develop a non-conducting sheath around electrode which prevents further electrical communication.

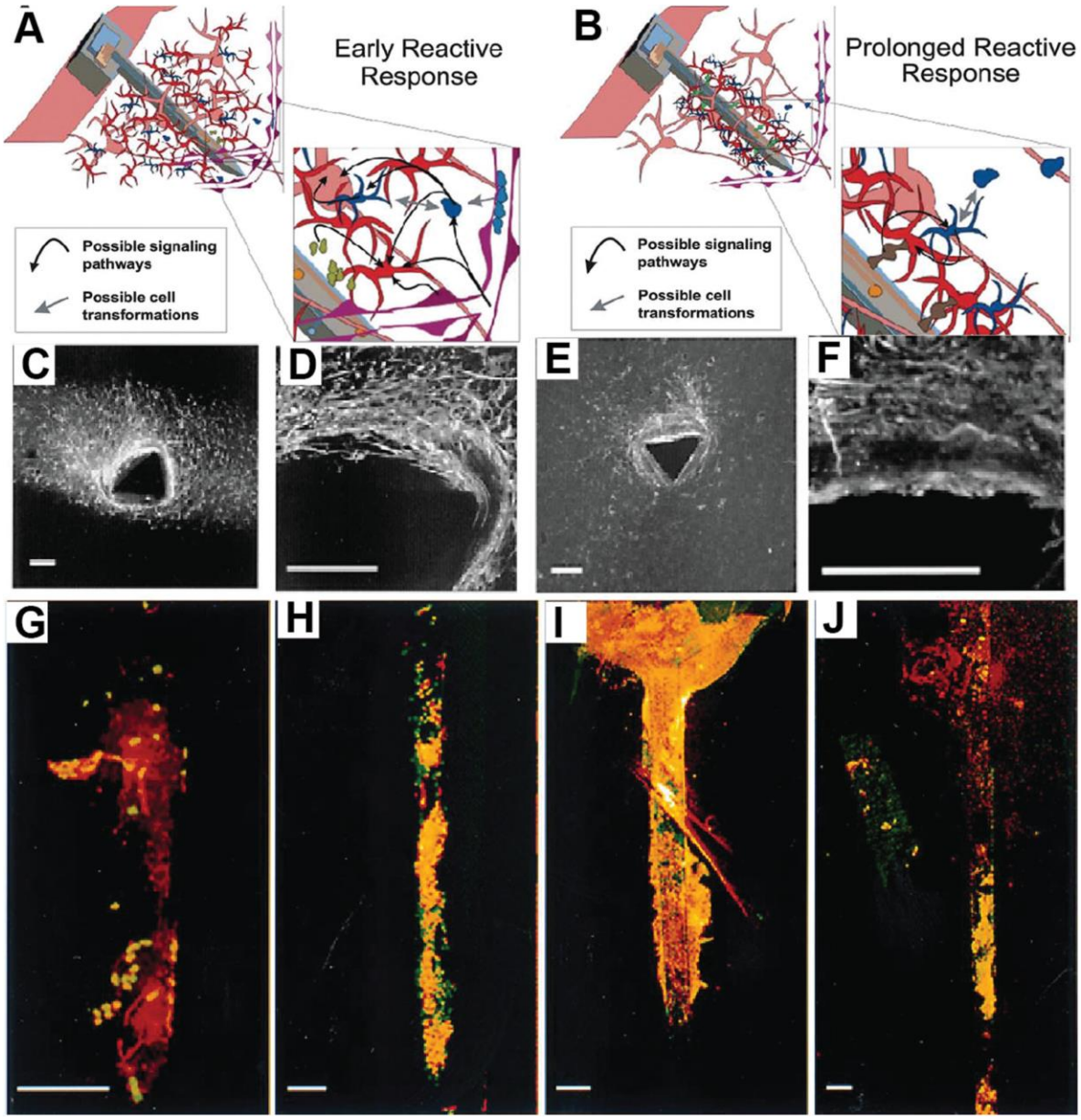

Figure 6. Schematics showing cellular response to neural-electrode insertion

Delocalized electrons along the polymer backbone and dopants which are also called mobile charge careers result in electrical conductivity of the CPs. The electrical conductivity of CPs is controlled by the level of doping. CPs can be synthesized by electrochemical polymerization and doped by counter ions for charge neutrality.

An important parameter that plays a significant role in recording electrodes is impedance which is related to SNR. CP's have been able to reduce impedance that increases SNR (21), which is highly desirable. In the case of stimulation devices, the need is to reduce the electrode size as much as possible in order to attain a densely packed array. However, decreasing the size of the electrode decreases charge-injection thereby reducing the stimulating capability of the metal electrode. As CP's like PEDOT and PPy have a high surface roughness, they have the capability to solve this problem by increasing the charge injection even with smaller electrode size (22). CP based materials are also gaining popularity for drug delivery applications (23). In addition to delivering charge, CP based microcapsules can deliver therapeutic molecules like drugs and growth factors etc. There are 3 ways for loading biomolecules in CPs: 1) as immobilized molecules covalently bonded within the polymer matrix (24) 2) as a mobile dopant that can be electrochemically delivered to target organs or tissues (25) 3) as an encapsulated molecule that can be driven out of the polymer by biodegradation of the polymer or some other techniques (26). Moreover, the incorporation of the molecule depends upon the application and mode of delivery. Finally, there is one more application of CPs in promoting neural regeneration (27) which is the main topic of this thesis.

1.4 Objective of the thesis

As stated earlier, ECM proteins like Laminin may single-handedly guide axonal growth by inducing direction sensitive movements in growth cones. Also, the potential of CPs in enhancing neural regeneration has been explained earlier. This thesis is

focused on fusing both the Laminin and CPs for neural regeneration applications. Moreover, the objective of the work conducted here is limited to the optimization of printing of Laminin droplets on the surface of CPs.

These were following objectives of the thesis: to obtain minimum void space between droplets, to make the patterns as small as possible, to remove any overlaps between droplets, to get minimum droplet volume for Laminin, to get a clear and consistent intensity, and to get a completely dark background. The following were the parameters needed to be optimized in order to attain desired objectives: Hamilton syringe size and type, volume of each droplet, horizontal and vertical distance between the droplets, the methods for preparing solutions, and the pattering strategy for printing Laminin.

CHAPTER 2. MATERIALS AND METHODS

2.1 Materials

Agarose was purchased from VWR Chemicals (Solon, Ohio). BSA (Fraction V, heat shock treated, molecular weight: 66.4kDa, pH - 7±0.3), Laminin from Engelbreth-Holm-Swarm murine sarcoma, Poly-L-lysine solution (Molecular weight range: 70 - 150kDa), and anti-Laminin antibody produced in rabbit – 0.5mg/ml all were purchased from Sigma-Aldrich (Saint Louis, Missouri).

2.2 Printing Laminin on conducting polymer

2.2.1 Preparation of conducting polymer substrates

The preparation of CP substrates consisted of three-steps: EVAP, substrate dicing, and electrodeposition. EVAP was done to create rectangle shaped gold-plated silicon substrates as shown in figure 7(A). Gold was added to the surface of Silicon wafer to increase its surface conductivity. During EVAP, a layer of Chromium was first added to surface of the Silicon wafer to improve the attachment of gold on silicon. After the EVAP treatment of gold-plated silicon disc, the substrates (Figure 7(A)) were diced out of the gold-plated silicon disc using a diamond tipped cutter. The substrates were then washed properly with DI water to remove any dust from the surface and then dried with nitrogen gas under pressure to ensure no debris or impurities were left on the surface.

After cleaning, the section between the part to be coated (part 2), and the part not to be coated (part 1) with polymer was painted with nail polish.

For the final stage, a monomer solution of 42.72µl of 0.2M EDOT & 824mg of 0.02M PSS in 20 ml DI water was prepared. The solution was then filled in an electrolytic cell as shown in the arrangement in figure 7(B). For electrodeposition, the substrate was clamped with an alligator clip to WE-SE end as shown in figure 7(B). The other end where a platinum coil was connected to CE-RE circuit provided counterions to balance the charges in electrolyte. In this manner, the electrolytic cell was connected to the Autolab (Figure 7(B)). After the part of the substrate that was to be coated (part 2) was properly dipped in the solution, the cell was turned on, and initial voltage was checked which should be in the range 0.3 – 0.5 V. Afterwards, the substrate was subjected to constant GSTAT deposition using Nova software leading to deposition of PEDOT polymer on the substrate surface. The golden color of the substrate surface soon turned to dark blue (Figure 8), which is the color of PEDOT polymer chains showing successful polymerization of EDOT monomers and their deposition on gold-plated substrates. The substrates were then washed with DI water, dried, and kept in 60 µl PLL solution as represented by brown colored covering over the substrate surface in figure 9. The 0.001% diluted PLL in DI water acted as an attachment agent and was added to increase Laminin retention on polymer surface. Each substrate was soaked with PLL for 10 minutes followed by gentle washing with DI water. The washed substrates were then either kept in an oven at 50^{o}C for 60 minutes or left at room temperature for overnight.

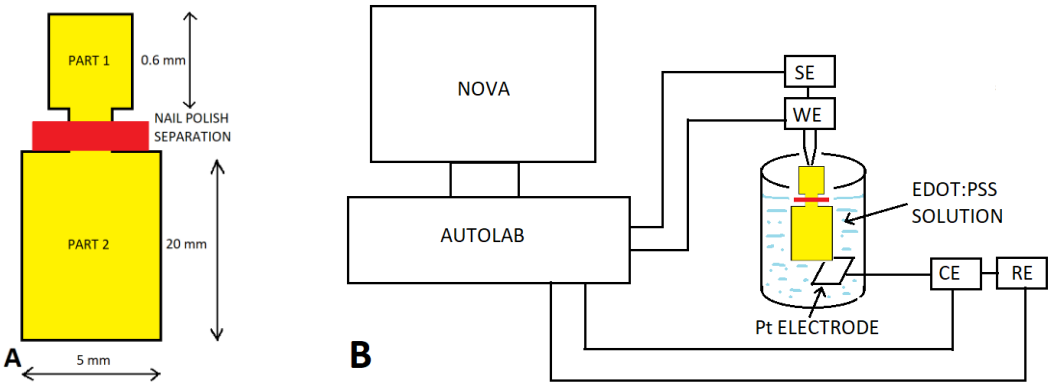

Figure 7. Schematic representation of (A) gold coated substrate, and (B) electrodeposition process

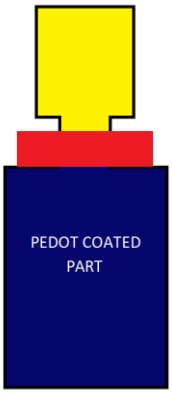

Figure 8. Schematic representation of PEDOT coated substrate

2.2.2 Preparation of Agarose hydrogel

Agarose powder was first dissolved at 2% w/v in DI Water in an Erlenmeyer flask. The solution was then heated in a microwave oven until a homogenous solution was obtained, i.e., no powder particles were visible in the solution anymore. The homogenous Agarose solution was then poured into a glass molds with a glass cover to cover the top surface to make sure that the surface of the hydrogel was smooth. The mold was then kept in refrigerator at 4^{o}C for 60 minutes. The mold was then brought

out at room temperature, glass cover was removed, and the mold was kept at room temperature for 20 minutes to get rid of surface water which gets evaporated.

Figure 9. PEDOT coated substrate soaked in 60µl PLL (brown)

2.2.3 Laminin printing and transferring to conducting polymer

After assuring the dryness of hydrogel surface, it was placed on the XYZ stage connected to the controller as shown in figure 10. A Hamilton syringe was clamped on the syringe holder connected to a syringe pump. A droplet was collected at the syringe tip and after making sure that a sufficiently sized droplet was generated, the droplet was deposited on the surface of the hydrogel. In the same manner the whole pattern was printed on the hydrogel. After the completion of printing, the CP was placed over the hydrogel for 7 minutes, and in this manner, the pattern was transferred to the CP.

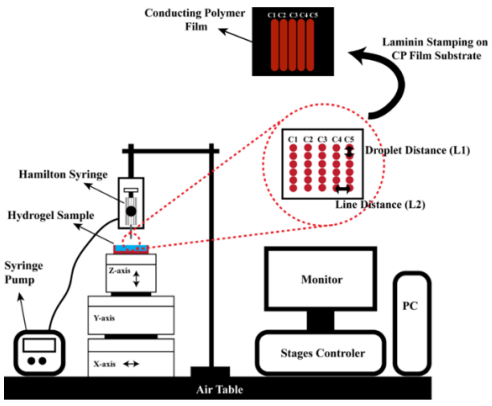

Figure 10. Schematic arrangement of XYZ stage for printing Laminin on hydrogel

2.3 Immunohistochemistry

After the pattern was transferred to the CP, the CP was subjected to a three-step immunohistochemistry process which consisted of treatment with BSA followed by treatment with primary and secondary antibodies, respectively. All the 3 solutions were prepared in the PBS. The CP with the Laminin pattern on it was soaked in 60 µl de-frozen BSA solution (Figure 11 (A)) for 30 minutes and then washed gently with DI water and dried with a tissue napkin. PAB solution was prepared by diluting PAB from the source with PBS in 1:30 volume ratio. The BSA treated substrate was then kept in the 60 µl freshly prepared PAB solution (Figure 11(B)) for either 60 minutes at room temperature, or for overnight in refrigerator at 4^{o}C, then washed with DI water and dried with a tissue napkin. SAB solution was prepared by diluting SAB from the source with PBS in 1:100 volume ratio. The PBS treated substrate was then soaked in freshly prepared SAB solution (Figure 11(C)) for 180 minutes in dark to avoid saturation of light sensitive SAB.

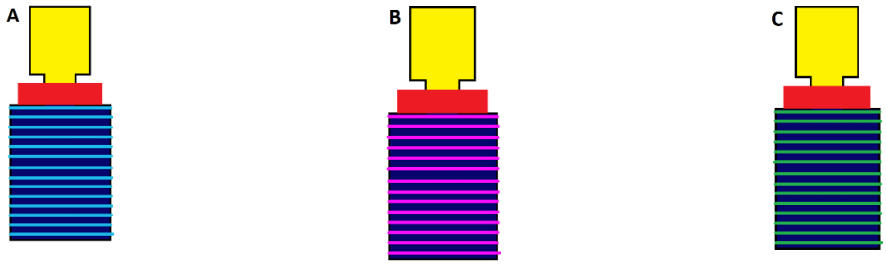

Figure 11. Schematic representation of soaking Laminin coated substrate in 60µl (A) BSA (blue), (B) PAB (violet), and (C) SAB (green)

CHAPTER 3. RESULTS AND DISCUSSIONS

Two types of Hamilton syringes were used for the experiments as listed in Table 1. At first, the syringe with gauge #30 was used with a droplet volume of 17.5nl (Table 2).

Table 1. Comparison of the two Hamilton syringes used for experiments

Gauge #	Outer Diameter (mm)	Inner Diameter (mm)	Minimum Droplet Volume (nl/s)	Droplet Diameter (µm)
30	0.312	0.159	10	800
34	0.159	0.051	5 and 3	350 and 500

Apparently, the block of Laminin as shown in figure 12 had a large droplet diameter, and an overlap between droplets. In order to resolve these problems, the syringe was checked for the minimum possible droplet volume that could be achieved without the droplet getting evaporated due to a very small volume. It was found that the minimum volume that could be obtained by the syringe was 10nl (Table 2). At 10nl droplet volume, 800µm horizontal distance, and 380µm vertical distance, desired results were obtained with a minimal overlap in the horizontal direction as shown in

figure 13. However, the intensity of Laminin droplets in all the lines (figure 13) were not consistent. Moreover, there appeared to be 2-circles instead of 1-circle in every Laminin droplet, the background was also not sufficiently dark, and there was still overlap in the vertical direction.

Table 2. Parameters for Hamilton syringe with gauge #30

Parameter	Initial values	Optimized values
Droplet volume (nl/s)	17.5	10
Droplet Diameter (µm)	950	800
Horizontal distance (µm)	600	830
Vertical distance (µm)	600	380

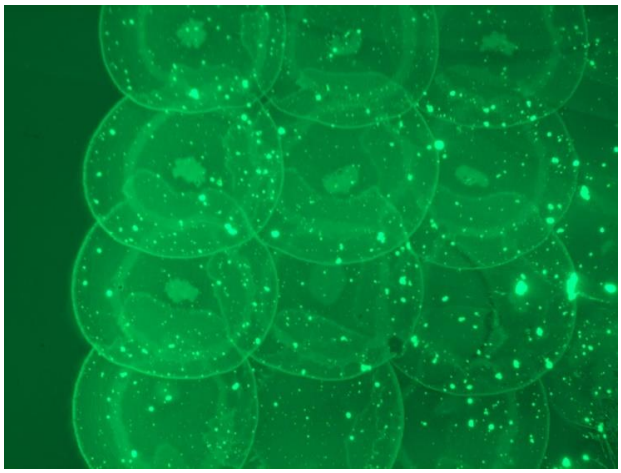

Figure 12. Laminin block (80µg/ml) with droplet volume of 17.5nl/s

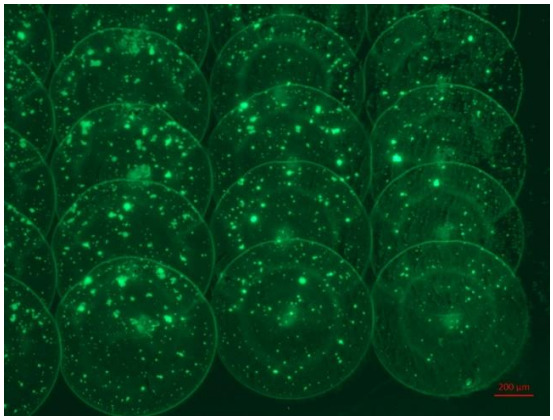

Figure 13. Laminin Block (80µg/ml) with droplet volume of 10nl/s

In order to resolve intensity related issues, we started taking Laminin from original stock as opposed to aliquots as done previously. In addition to this, we started using a new syringe with gauge #34 (Table 3) with a narrower needle. The minimum volume of the Laminin droplet that could be achieved with this syringe was 5nl. Experiments were conducted to check the droplet diameter on CP so that the horizontal and vertical distances between droplets could be finalized. Figure 14 shows the results of these experiments. Various sets of horizontal and vertical distances were used. Finally, 2-sets were chosen for comparison (Figure 15), the second set with horizontal and vertical distances of 440µm and 350µm, respectively, and the last set with horizontal and vertical distances of 440µm and 200µm, respectively. The main reason behind selecting these two sets for comparison was that the second set had droplets with no overlap, whereas, the last set had droplet overlaps but consumed less space which could improve the pattern resolution by a good amount. Lastly, the second set of patterns was chosen as a standard to decide the horizontal and vertical distances between droplets as this pattern gave us the actual droplet diameter and had no overlap which means there was only one concentration throughout the patterning.

Overlaps mostly consist of multiple concentrations as is in the case of third, fourth, and fifth sets. The average droplet diameter for droplets in the second set was around 330µm. Based on the conclusions from this experiment, the droplet volume was fixed at 350µm, which approximately would have given patterns with no overlap and possibly minimum to no gaps between droplets in both horizontal and vertical directions.

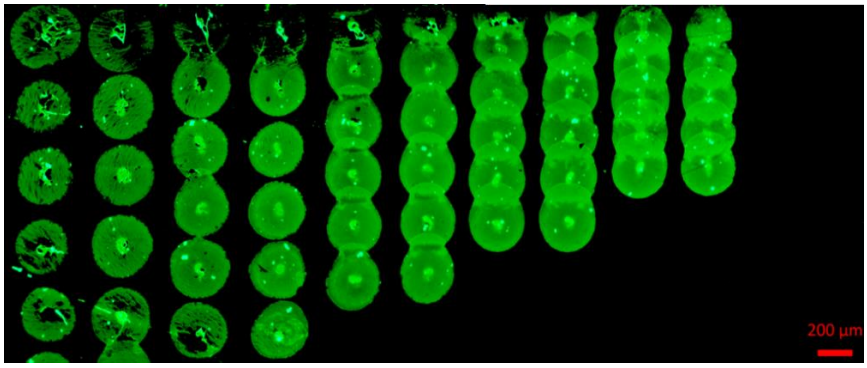

Figure 14. Laminin block (100µg/ml) with different distances between droplets

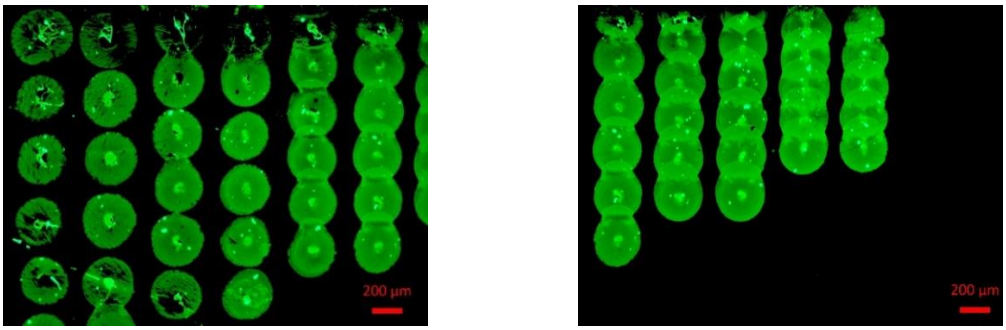

(A) (B)

Figure 15. Block of laminin (100µg/ml) showing (A) non-overlapping droplets, and (B) overlapping droplets

The shortlisted parameters were then tested to give results as shown in figure 16. The obtained average droplet diameter for these parameters was 380µm, standard deviation for the droplet diameter was 39.20µm, average absolute intensity of the droplets was 4065.77AU, and standard deviation for the droplet intensity was 531.64

AU. After doing further statistical analysis, it was found that there were 7 outlier droplets in terms of droplet diameter. After removing these droplets from the calculations, the average droplet diameter dropped to 369.47µm with a standard deviation of 3.39, and the intensity also fell to 4020.56AU with a standard deviation of 463.46AU. The final overall calculations for this pattern showed promising results, however, this pattern was non-uniform in terms of droplet diameter due to the presence of numerous outliers. Also, the Laminin intensity values were very low than expected, and it seems like the Laminin wasn't properly distributed in most of the droplets.

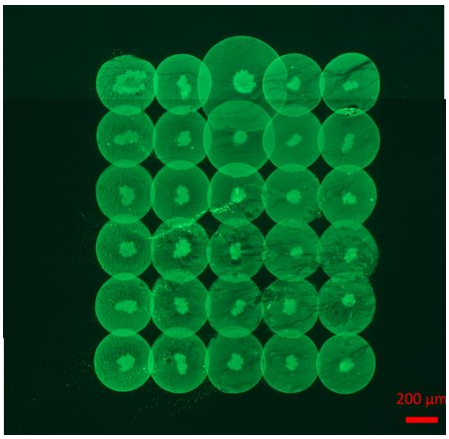

(A)

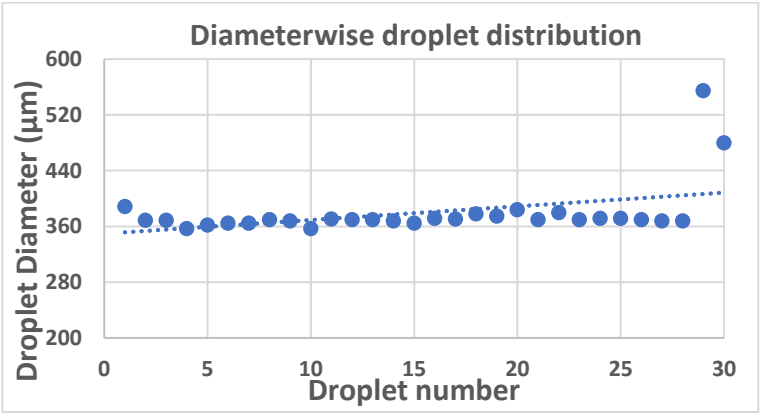

(B)

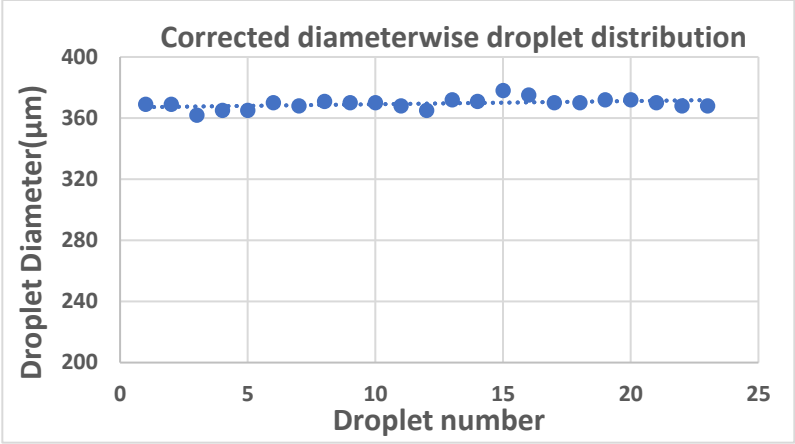

(C)

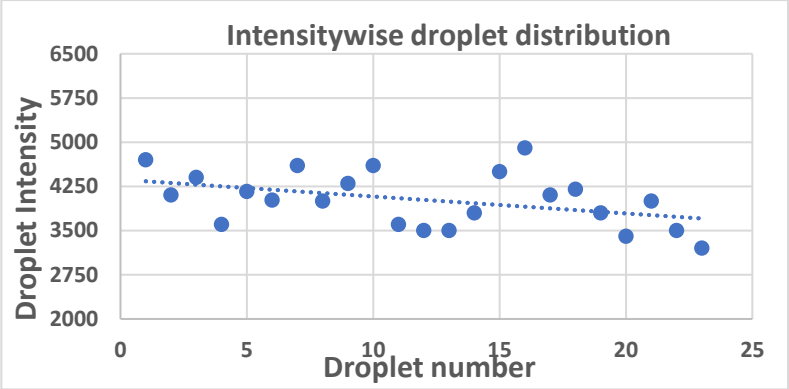

(D)

Figure 16. Laminin block (100µg/ml) with (A) a pattern, (B) diameter distribution, (C) corrected diameter distribution, and (D) intensity distribution for an Edge to Edge patterning

Therefore, this experiment needed to be repeated as shown in figure 17. This time 30 droplets were deposited in 2 arrays of 3×5 droplets per array in order to get a better and detailed data. The pattern was very consistent both in terms of the droplet diameter and the droplet intensity and no outliers were found. The average droplet diameter for 30 droplets was 342.27µm, the standard deviation for the droplet diameter was 11.06µm, the average absolute droplet intensity was 6956AU, and the standard deviation for the droplet intensity was 588.35AU. As there were no outliers

here, and the intensity values were high, this turned out to be the best obtained pattern for Edge to Edge patterning.

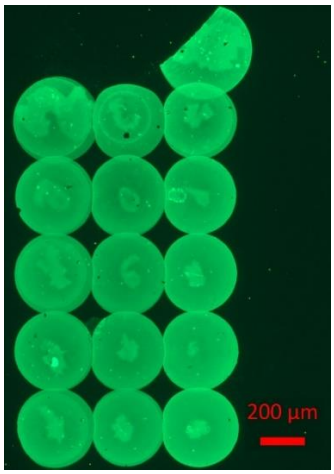

(A)

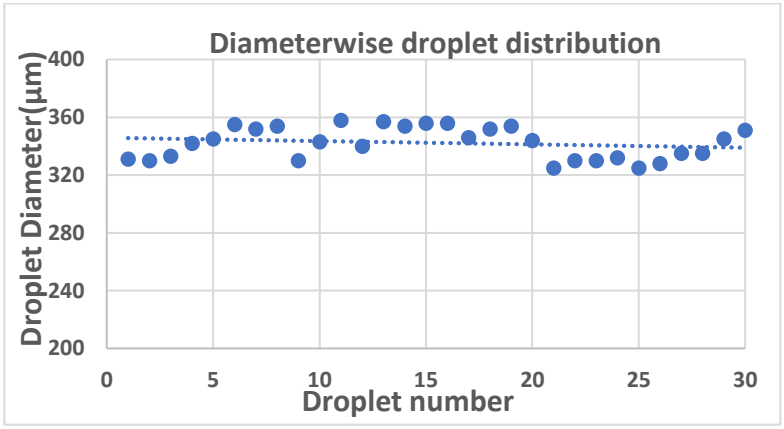

(B)

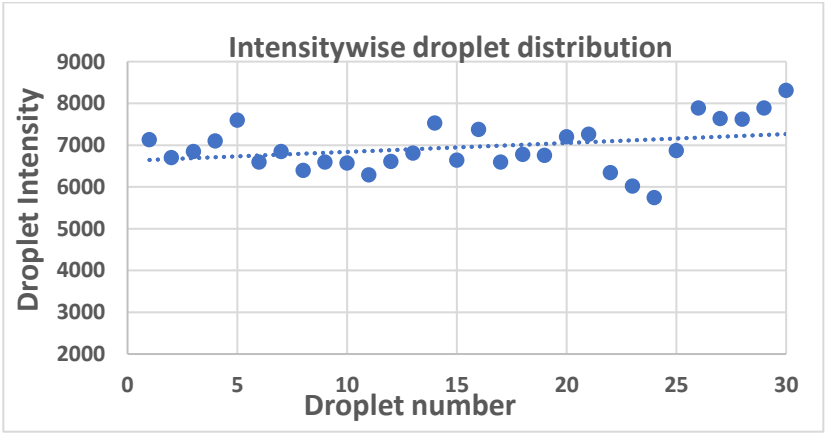

(C)

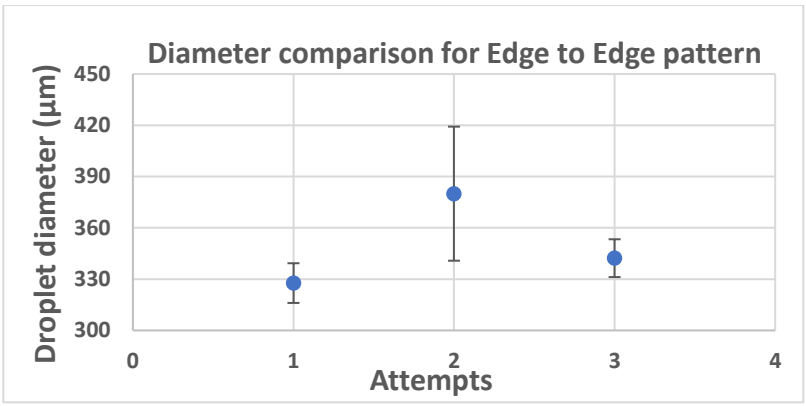

(D)

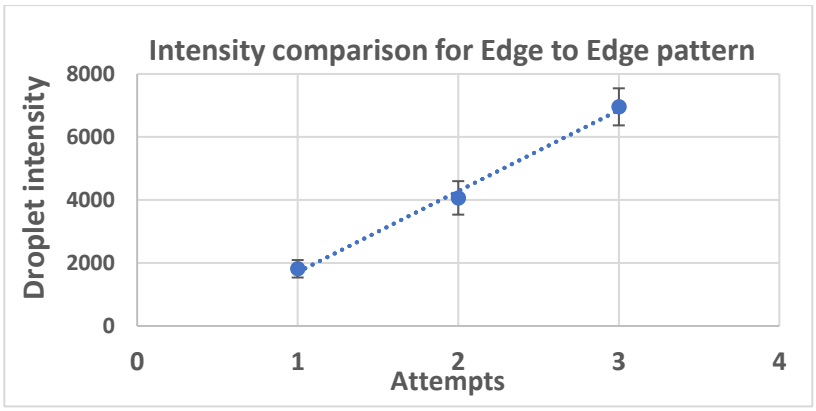

(E)

Figure 17. Laminin block (100µg/ml) with (A) pattern, (B) diameter distribution, (C) intensity distribution, (D) diameter comparison among patterns, and (E) intensity comparison among patterns for an Edge to Edge patterning

The next challenge was to decrease the void or dead space between the droplets to reduce the non-active space. This would be very helpful in avoiding any discontinuities in the path of regenerating neurons. In order to achieve minimum dead space, a new Shifted pattern technique was tried. As can be seen in figure 18, the basic idea was to shift every alternate line in the pattern by a distance equal to half of the standard droplet diameter i.e. 175µm in vertical direction.

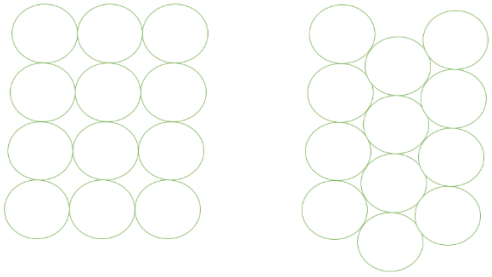

(A) (B)

Figure 18. Pictorial representation of (A) Edge to Edge, and (B) Shifted patterning techniques

An experiment was conducted to check the applicability of Shifted patterning, and results were obtained as shown in figure 19. This pattern turned out to be a very irregular one as it had 7 outlier droplets in terms of droplet diameters. After removing outlier droplets from data, an average droplet diameter of 355.37 µm, and an average absolute intensity of 5959.26AU was obtained. However, this pattern needed to be repeated as it had many irregularities in droplet deposition. Therefore, results were obtained from the next experiment as shown in figure 20. In this experiment, a very uniform pattern was obtained with an average droplet diameter of 347. 23µm, and an average absolute intensity of 6228.68AU, the intensity was good overall for this pattern. Also, the droplet diameter was very consistent throughout as it had a small standard deviation of 6.23µm only.

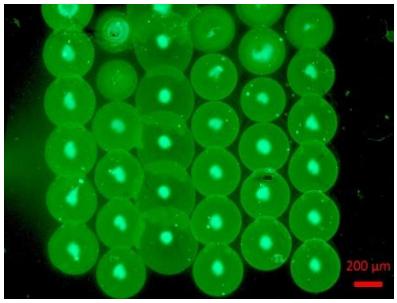

(A)

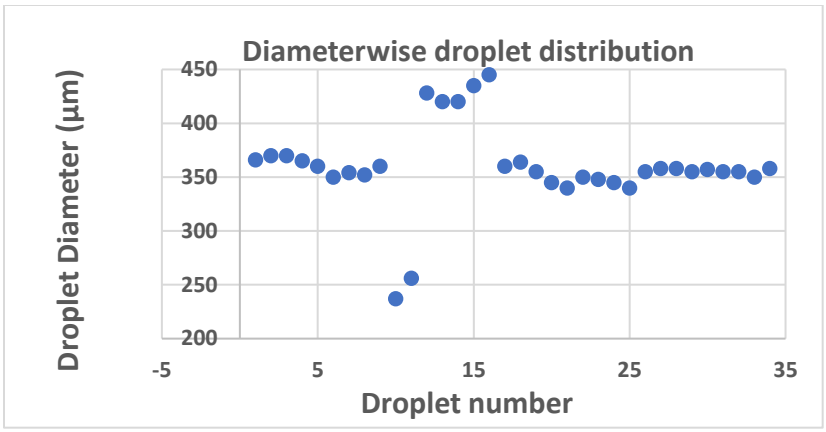

(B)

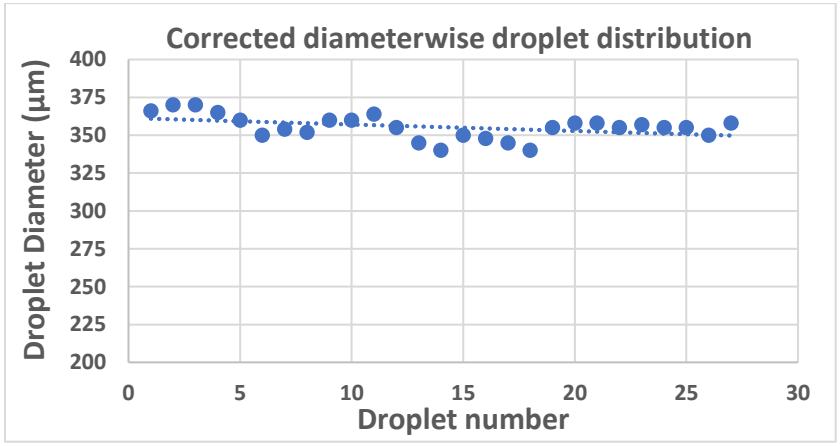

(C)

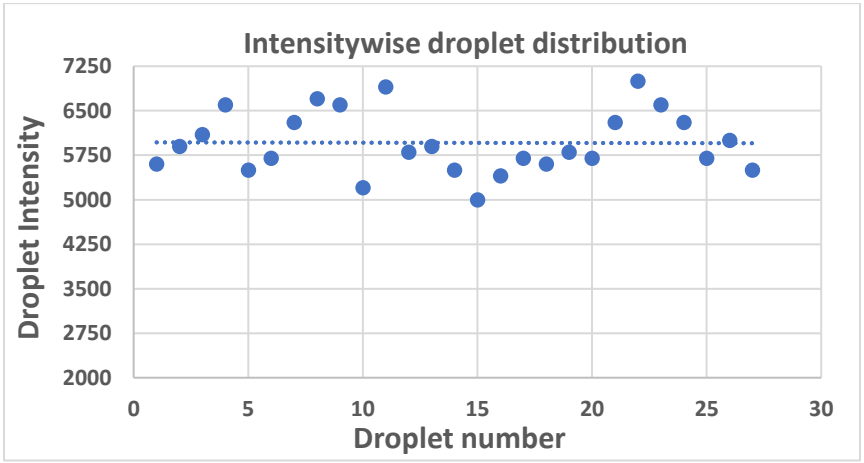

(D)

Figure 19. Laminin block (100µg/ml) with (A) a pattern, (B) diameter distribution, (C) corrected diameter distribution, and (D) intensity distribution for the Shifted patterning

This was a very properly deposited Shifted pattern (figure 20) except that there was no contact among the vertical lines in the horizontal direction. Consequently, there was a lot of void space between the droplets. The reason behind this was that the horizontal distance was still 350µm, however, it needed to be less than that as now there was no edge to edge contact, but instead the droplets needed to be closer in order to have a contact.

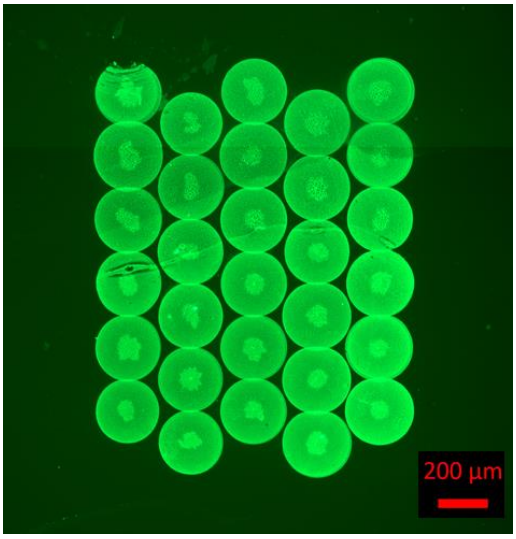

(A)

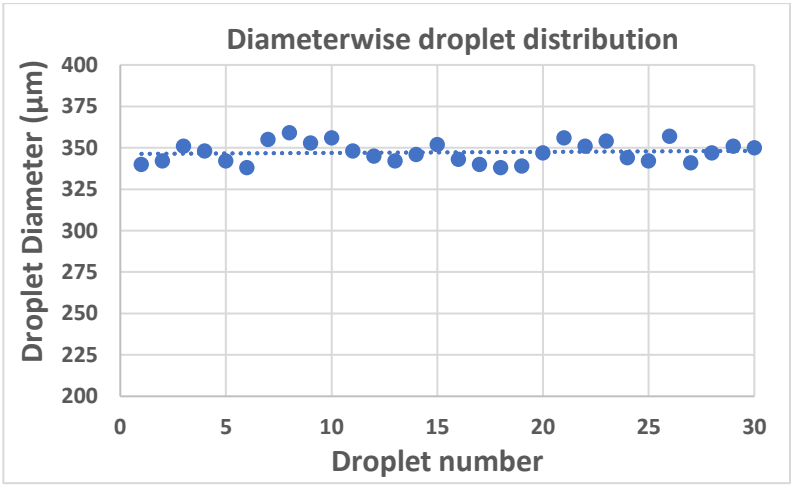

(B)

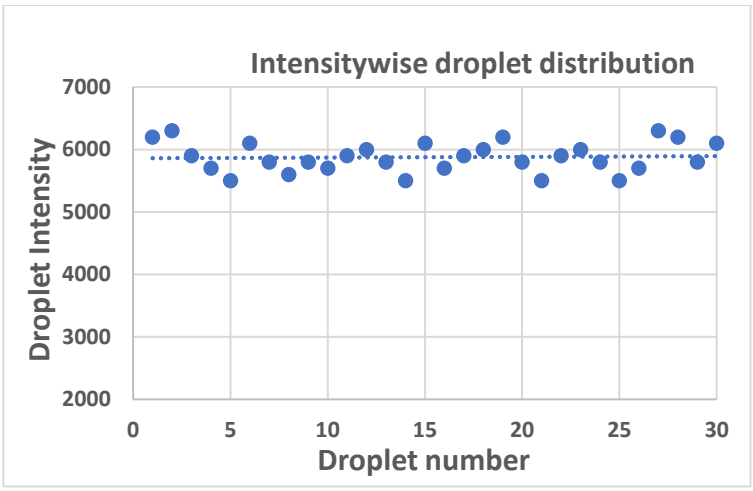

(C)

Figure 20. Laminin block (100µg/ml) with (A) a pattern, (B) diameter distribution, and (C) intensity distribution for the Shifted patterning

After a series of experiments, some changes were made to the distances. The vertical distance between the droplets was kept the same at 350µm, and the horizontal distance was optimized to 330µm. The results were obtained as shown in figure 21. Overall, the pattern seemed promising with a good presentation of Shifted patterning with only one outlier in terms of droplet diameter. The average diameter for this pattern after the removal of the outlier droplet was 364.72µm with a very narrow standard deviation of 3.81µm showing the perfection of patterning. Also, the average absolute intensity after removing the outlier droplet was 5804. An experiment showed that the minimum droplet volume that could be obtained by the syringe with gauge #30 was 3nl when a shorter needle was used. The reason behind this may have been a better flow through the shorter needle. Moreover, experiments were conducted to see what droplet diameter could be obtained with the 3nl Laminin droplet. Results showed that the diameter of droplets that could be obtained by 3nl droplet was 500µm.

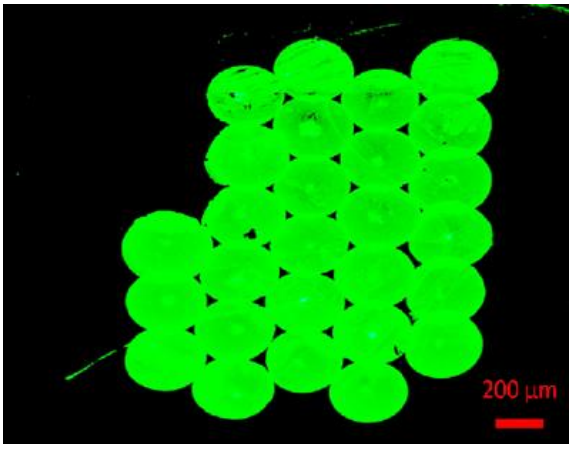

(A)

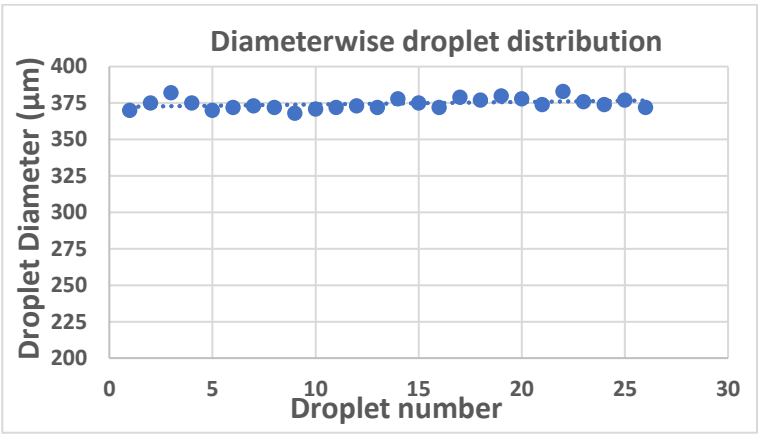

(B)

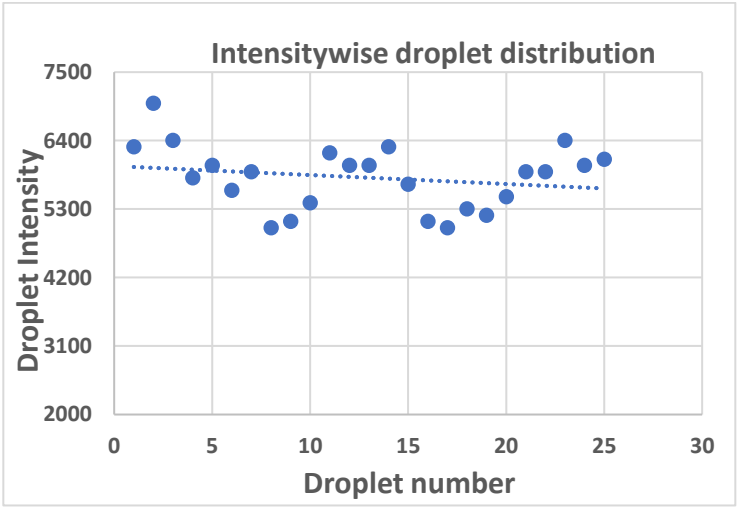

(C)

Figure 21. Laminin block (100µg/ml) with (A) a pattern, (B) diameter distribution, and (C) intensity distribution for the Shifted patterning

More experiments were conducted to see what horizontal and vertical distances would be appropriate to make a Shifted pattern of Laminin deposition. Figure 22 shows a result from an experiment presenting a perfectly deposited Shifted pattern. The average droplet diameter for this pattern was 506.80µm with a standard deviation of 4.48µm which showed the uniformity of the deposition. The average absolute intensity for the droplets was 6330 which again was pretty much in line with what had been obtained.

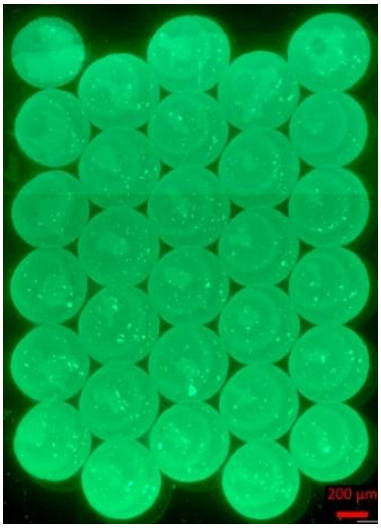

(A)

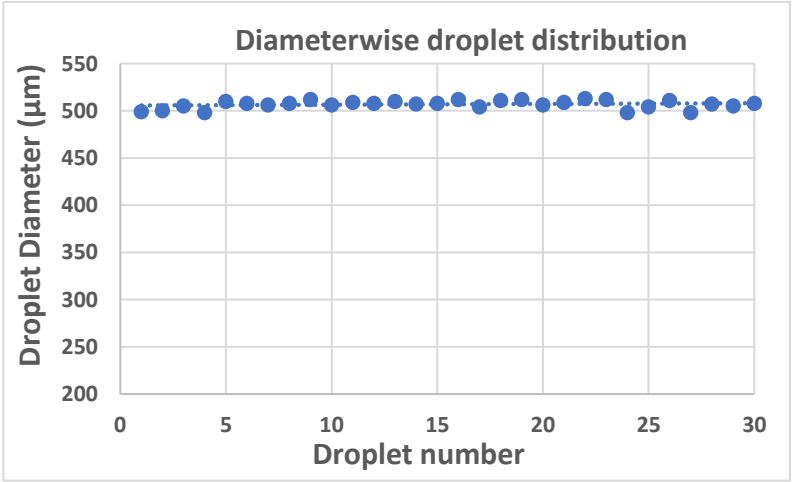

(B)

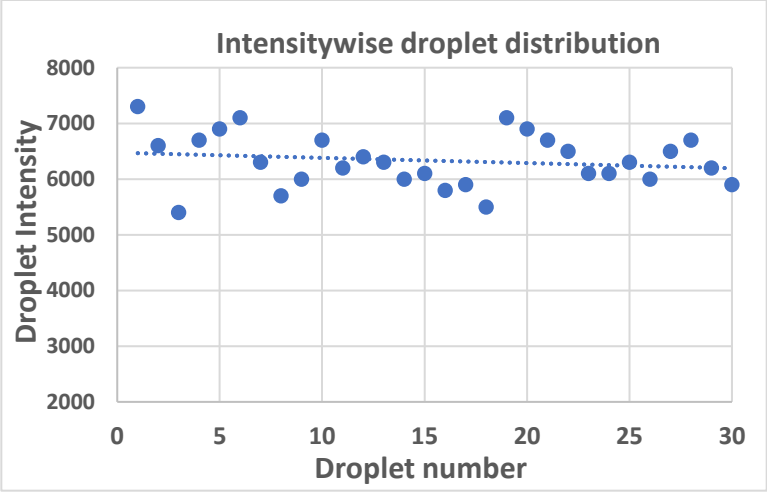

(C)

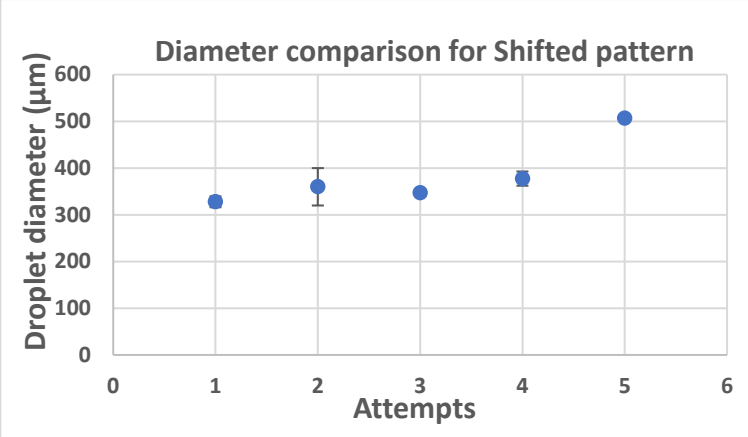

(D)

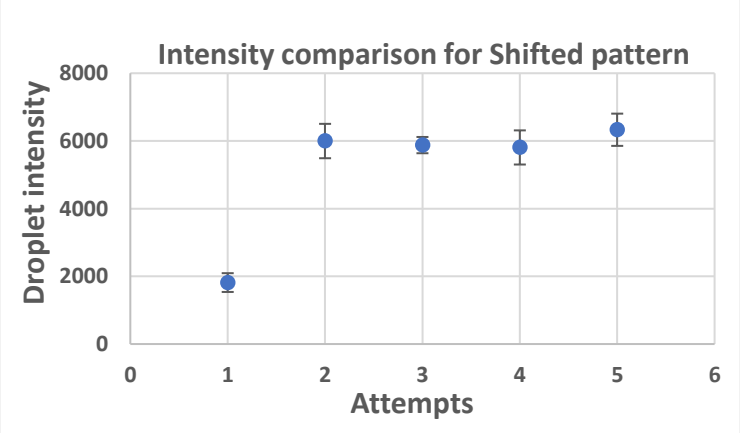

(E)

Figure 22. Laminin block (100µg/ml) with (A) a pattern, (B) diameter distribution, and (C) intensity distribution, (D) diameter comparison, and (E) intensity comparison for the Shifted patterning

So far, this was the best obtained and optimized pattern in terms of droplet diameter, droplet intensity, droplet volume, and void space. Figure 23 shows what benefits this pattern had over the Edge to Edge pattern of same surface area. A square and a parallelogram were made joining the centers of the circles in the two patterns, respectively. It's interesting to note that the void space in the Edge to Edge pattern was 21.5% of the area of the square, whereas, the void space was only 9.29% of the area of the parallelogram in the Shifted pattern. To support the fact that Shifted pattern had less void space between the droplets, measurements were taken, and it was found that the horizontal distance between the droplets had reduced to around 350µm against 500µm as was in the case of Edge to Edge patterning. Finally, an attempt was made to employ the parameters finalized for the Shifted pattern to make Laminin gradients as shown in figure 24. The major difference between the previous patterns and this one was that the syringe needed to be refilled and changed every time a different concentration was to be deposited. However, the patterns had an average droplet diameter of 505.83µm and standard deviation of 5.06µm which again showed that the pattern was very well deposited.

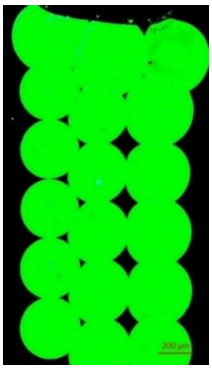

(A)

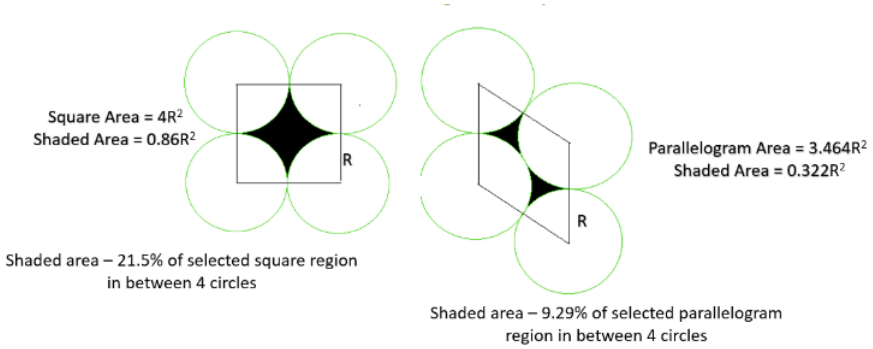

(B)

Figure 23. Representation of difference between the two types of pattering in terms of (A) laminin patterns, and (B) pictorial representations

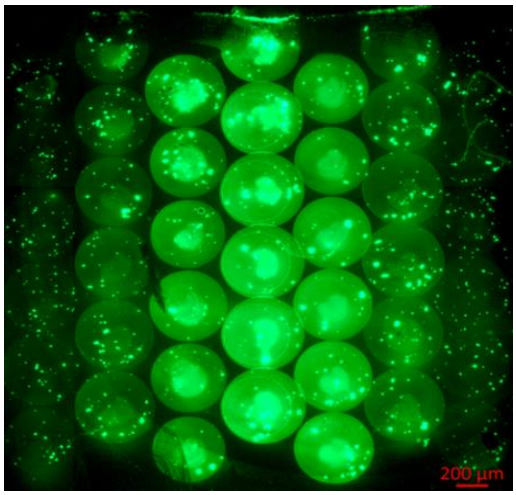

(A)

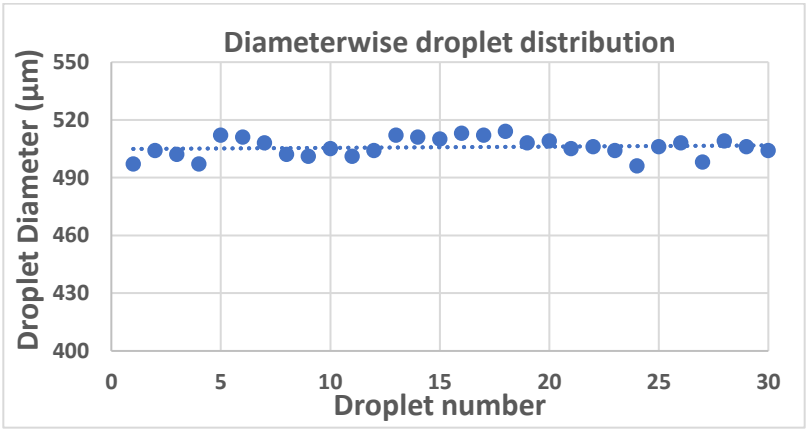

(B)

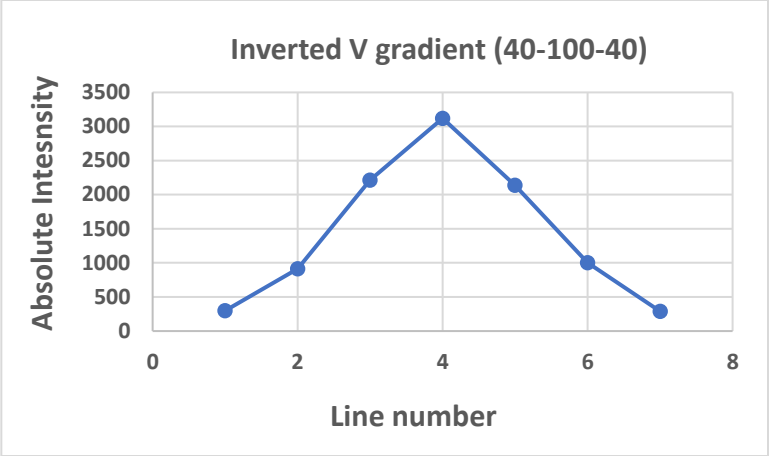

(C)

Figure 24. (A) Inverted-V Laminin gradient (40-60-80-100-80-60-40µg/ml), (B) droplet diameter range, and (C) graph representing intensities in Laminin gradient for the Shifted patterning

The concentration of the profile was very low as compared to the previous block-based attempts, but the inverted V type gradient was still very clearly visible as shown in figure 24. In all the Laminin block patterns above, trendline was used to indicate non-dependence of droplet or diameter on droplets. The lower values of R^2 in all the results except in figure 17(D), and figure 22(D)-(E) showed there was no or negligible change in the diameter and intensity of droplets throughout the pattern. In figure 17(D), R^2 value of 0.99 showed that the intensity, and hence quality of deposited Laminin increased with every experiment for Edge to Edge patterning. Similarly, R^2 value of 0.52 in figure 22(D) showed a decent increase in quality of Laminin deposition with every experiment for Shifted patterning.

CHAPTER 4. CONCLUSIONS AND FUTURE WORK

In this study, Laminin, an ECM protein, was deposited on the surface of a CP in two types of patterning arrangements, an Edge to Edge patterning, and a Shifted patterning. In the Edge to Edge patterning, the droplets in the pattern had an edge to edge contact with each other both in horizontal and vertical directions, whereas, in the shifted patterning, alternate lines were shifted by a distance equal to half of the diameter so that the void space can be minimized. Throughout the study, different parameters were optimized to decrease the droplet volume for Laminin droplet, to idealize the horizontal and vertical distances between droplets, to increase the intensity of droplets, and to minimize the void space between droplets. The volume of each droplet was decreased from 17.5nl to 10nl to 5nl, and finally to 3nl. The horizontal and vertical distances between the droplets were both initially 830µm. Both the horizontal and vertical distances were brought down to 350µm for the Edge to Edge patterning. For the Shifted patterning, the horizontal and vertical distances were brought down to 500 and 450µm, respectively. The absolute intensity of Laminin was increased from an initial value of around 2000 to around 6000. Shifted patterning technique was sought out as an alternative to the previously being used Edge to Edge patterning technique to decrease the void space between droplets. It was concluded that the Shifted patterning decreased the horizontal distance between lines by approximately 30%. At last, the parameters that were finalized for block type patterning were employed to see their applicability in depositing Laminin gradients on CPs. With the initial success, the future

studies will be focused on exploiting whatever has been achieved to make longer Laminin blocks and gradients. Also, the future projects include testing of these Laminin coated CP substrates to see the response of actual neurons for neural regeneration applications.

REFERENCES

1. Dickson, B. J. (2002). Molecular Mechanisms of Axon Guidance. *Science*, *298*(5600), 1959-1964.
2. Baier, H., & Bonhoeffer, F. (1994). Attractive Axon Guidance Molecules. *Science*, *265*(5178), 1541-1543.
3. Lumsden, A. G. S., & Davies, A. M. (1983). Earliest Sensory Nerve Fibres are Guided to Peripheral Targets by Attractants Other than Nerve Growth Factor. *Nature*, *306*(5945), 786.
4. Serafini, T., Kennedy, T. E., Gaiko, M. J., Mirzayan, C., Jessell, T. M., & Tessier-Lavigne, M. (1994). The Netrins Define a Family of Axon Outgrowth-Promoting Proteins Homologous to C. Elegans UNC-6. *Cell*, *78*(3), 409-424.
5. Gundersen, R. W., & Barrett, J. N. (1979). Neuronal Chemotaxis: Chick Dorsal-Root Axons Turn Toward High Concentrations of Nerve Growth Factor. *Science*, *206*(4422), 1079-1080.
6. Kennedy, T. E., Serafini, T., de la Torre, J., & Tessier-Lavigne, M. (1994). Netrins are Diffusible Chemotropic Factors for Commissural Axons in the Embryonic Spinal Cord. *Cell*, *78*(3), 425-435.
7. Hedgecock, E. M., Culotti, J. G., & Hall, D. H. (1990). The Unc-5, Unc-6, And Unc-40 Genes Guide Circumferential Migrations of Pioneer Axons

and Mesodermal Cells on the Epidermis in C. Elegans. *Neuron, 4*(1), 61-85.

8. Gundersen, R. W., & Barrett, J. N. (1980). Characterization of the Turning Response of Dorsal Root Neurites Toward Nerve Growth Factor. *The Journal of cell biology, 87*(3), 546-554.

9. Letourneau, P. C. (1975). Cell-To-Substratum Adhesion and Guidance of Axonal Elongation. *Developmental biology*, *44*(1), 92-101.

10. Heidemann, S. R., Lamoureux, P., & Buxbaum, R. E. (1990). Growth Cone Behavior and Production of Traction Force. *The Journal of cell biology*, *111*(5), 1949-1957.

11. O'Connor, T. P., Duerr, J. S., & Bentley, D. (1990). Pioneer Growth Cone Steering Decisions Mediated by Single Filopodial Contacts in Situ. *Journal of Neuroscience*, *10*(12), 3935-3946.

12. Rajagopalan, S., Vivancos, V., Nicolas, E., & Dickson, B. J. (2000). Selecting a Longitudinal Pathway: Robo Receptors Specify the Lateral Position of Axons in The Drosophila CNS. *Cell*, *103*(7), 1033-1045.

13. Swindle-Reilly, K. E., Papke, J. B., Kutosky, H. P., Throm, A., Hammer, J. A., Harkins, A. B., & Willits, R. K. (2012). The Impact of Laminin on 3D Neurite Extension in Collagen Gels. *Journal of neural engineering*, *9*(4), 046007.

14. Wu, T., Li, D., Wang, Y., Sun, B., Li, D., Morsi, Y., ... & Mo, X. (2017). Laminin-Coated Nerve Guidance Conduits Based on Poly (L-Lactide-Co-

Glycolide) Fibers and Yarns for Promoting Schwann Cells' Proliferation and Migration. *Journal of Materials Chemistry B*, *5*(17), 3186-3194.

15. Haggerty, A. E., Al-Ali, H., & Oudega, M. (2018). Soluble Laminin Polymers Enhance Axon Growth of Primary Neurons In Vitro. *Journal of Biomedical Materials Research Part A*, *106*(9), 2372-2381.

16. Dertinger, S. K., Jiang, X., Li, Z., Murthy, V. N., & Whitesides, G. M. (2002). Gradients of Substrate-Bound Laminin Orient Axonal Specification of Neurons. *Proceedings of the National Academy of Sciences*, *99*(20), 12542-12547.

17. Xiao, R. R., Zeng, W. J., Li, Y. T., Zou, W., Wang, L., Pei, X. F., ... & Huang, W. H. (2013). Simultaneous Generation of Gradients with Gradually Changed Slope in a Microfluidic Device for Quantifying Axon Response. *Analytical chemistry*, *85*(16), 7842-7850.

18. Branch, D. W., Corey, J. M., Weyhenmeyer, J. A., Brewer, G. J., & Wheeler, B. C. (1998). Microstamp Patterns of Biomolecules for High-Resolution Neuronal Networks. *Medical and Biological Engineering and Computing*, *36*(1), 135-141.

19. Joddar, B., Guy, A. T., Kamiguchi, H., & Ito, Y. (2013). Spatial Gradients of Chemotropic Factors from Immobilized Patterns to Guide Axonal Growth and Regeneration. *Biomaterials*, *34*(37), 9593-9601.

20. Fricke, R., Zentis, P. D., Rajappa, L. T., Hofmann, B., Banzet, M., Offenhäusser, A., & Meffert, S. H. (2011). Axon Guidance of Rat Cortical

Neurons by Microcontact Printed Gradients. *Biomaterials*, *32*(8), 2070-2076.

21. Wark, H. A. C., Sharma, R., Mathews, K. S., Fernandez, E., Yoo, J., Christensen, B., & Tathireddy, P. (2013). A New High-Density (25 electrodes/mm2) Penetrating Microelectrode Array for Recording and Stimulating Sub-Millimeter Neuroanatomical Structures. *Journal of neural engineering*, *10*(4), 045003.

22. Ludwig, K. A., Uram, J. D., Yang, J., Martin, D. C., & Kipke, D. R. (2006). Chronic Neural Recordings Using Silicon Microelectrode Arrays Electrochemically Deposited With a Poly (3, 4-ethylenedioxythiophene)(PEDOT) Film. *Journal of neural engineering*, *3*(1), 59.

23. Abidian, M. R., & Martin, D. C. (2009). Multifunctional Nanobiomaterials for Neural Interfaces. *Advanced Functional Materials*, *19*(4), 573-585.

24. Abidian, M. R., Kim, D. H., & Martin, D. C. (2006). Conducting-Polymer Nanotubes for Controlled Drug Release. *Advanced materials*, *18*(4), 405-409.

25. Green, R. A., Lovell, N. H., & Poole-Warren, L. A. (2009). Cell Attachment Functionality of Bioactive Conducting Polymers for Neural Interfaces. *Biomaterials*, *30*(22), 3637-3644.

26. Massoumi, B., & Entezami, A. (2002). Electrochemically Controlled Binding and Release of Dexamethasone from Conducting Polymer

Bilayer Films. *Journal of bioactive and compatible polymers*, *17*(1), 51-62.

27. Thompson, B. C., Moulton, S. E., Ding, J., Richardson, R., Cameron, A., O'Leary, S., & Clark, G. M. (2006). Optimising the Incorporation and Release of a Neurotrophic Factor Using Conducting Polypyrrole. *Journal of Controlled Release*, *116*(3), 285-294.